Progress of Theoretical Physics, Vol. 57, No. 6, June 1977

Nonlinear Fluctuations Associated with Instabilities in Dissipative Systems

Ki-ichi NAKAMURA

Central Research Laboratories, Nippon Electric Co. Ltd., Kawasaki 213

(Received November 25, 1976)

Computer experiments are performed on a model system of coupled mode equations designed to represent the Gunn instability, in order to investigate the origin of anomalously large fluctuations observed often over a wide range beyond an instability point in a dissipative system. The experiments deal with a system of 40 modes which possesses a number of steady states (attractors) beyond the instability point. It is shown that the system travels in phase space along an erratic or chaotic trajectory for long time in the approach to one of these attractors from an unstable equilibrium point. According to the modern ergodic theory, trajectories are proved to be stochastic by demonstrating that they satisfy the exponential law of growth of stochastic instability, that is, they are unstable with respect to small disturbances. The system provides an example of rigidly deterministic systems whose dynamics are best described in stochastic terms. It is found that under the influence of random forces the system escapes from the reached attractor after fluctuating around it for some time and travels again along a long-lived stochastic trajectory. The system wanders erratically from attractor to attractor via macroscopically stochastic trajectories, which do not arise from external random forces, but from the nonlinearity inherent in the system. This wandering motion is observed as large fluctuations.

§ 1. Introduction

A dissipative system often exhibits anomalously large fluctuations over a wide range beyond an instability point. A typical example is fluid turbulence. The root mean squares of the fluctuations in the velocity of water in turbulent flow through a tube become anomalously large beyond the critical Reynolds number.[1] Similar behavior is observed in the fluctuation phenomena of various physical quantities: the Nusselt number in a horizontal liquid helium layer heated below,[2] the local radial velocity in a fluid rotating between concentric cylinders,[3] the scattered (transmitted) intensity of neutron (light) in nematic liquid crystals,[4),5] the current noise due to the Gunn instability[6),7] or the acoustoelectric instability,[8),9] and the output intensity from junction lasers.[10] These experiments suggest that the occurrence of large fluctuations over a wide range is characteristic of instabilities in dissipative systems, in contrast with the critical fluctuations in the close vicinity of a phase transition point in an equilibrium system.

Lorenz[11] solved numerically a set of three differential equations designed to represent the Rayleigh-Bénard convection and discovered nonperiodic solutions of chaotic type beyond the critical Rayleigh number. These solutions are unstable

with respect to small modifications, so that slightly differing initial states can evolve into considerably different states. This feature is identical with that of stochastic instability, which leads to mixing and other statistical properties of motion, according to modern ergodic theory.[12)~14)] Lorenz thought that turbulence might be described by nonperiodic solutions. These solutions were named later "strange attractors" by Ruelle and Takens.[15)] Recently three more examples of strange attractors have been demonstrated by McLaughlin and Martin[16)] and Rössler.[17),18)] Since the nonperiodic solutions of chaotic type are obtained without introducing external stochastic elements into the basic equations, the motion described by them is macroscopic, so that it may be observed as large fluctuations.

In this paper, we propose an alternative mechanism for anomalous fluctuations on the basis of the results of computer experiments on the Gunn instability. In § 2 coupled mode equations are set up to model the Gunn instability in a one-dimensional case. Our computations deal with a system of 40 modes. The readers who are not interested in the derivation of the equations may skip a large part of § 2 and go to Eqs. (13). In § 3 we report the numerical results. Beyond the instability point, at which an equilibrium point becomes unstable, our system possesses a number of attracting fixed points and attracting closed orbits. These will be called sometimes "attractors" hereafter. It will be shown that the system travels in phase space along a long-lived erratic trajectory to reach one of these attractors from the unstable equilibrium point. It will be seen also that these trajectories satisfy the exponential law of growth of stochastic instability,[12)~14)] according to which initially close trajectory pair separates exponentially with time. Thus, our system provides an example of fully deterministic systems whose dynamics are best described probabilistically. Dissipative systems are always exposed by random forces through contact with a heat reservoir (or environmental causes). Our numerical experiments will show that if initial conditions are the same each other, at the early stage a system exposed by random forces travels along almost the same trajectory as that of a system without them, but after some time two trajectories begin to separate from each other, and at the later stage exhibit completely different paths. This means that the influence of random forces accumulated gradually on the system during its travel along the trajectory provokes an unexexcted behavior of the system after some time. Thus, one will see that under the application of external random forces the system escapes from the attractor after fluctuating around it for some time, and begins to travel again along a long-lived stochastic trajectory; the system wanders erratically from attractor to attractor via long-lived stochastic trajectories. This wandering motion looks seemingly like a strange attractor in a sense that there is no stable point to stay eternally. This motion will be observed as large fluctuations, because the motion itself is provoked by random forces, but its stochasticity is caused by the nonlinearity inherent in the system, in contrast with the thermal fluctuations in equilibrium systems. In the last section, we state our conclusions.

§ 2. Dynamical system representing the Gunn instability

We consider the Gunn instability in a one-dimensional case, which is governed by the following equation[19] for the electric field $E(x, t)$:

$$\frac{\partial E}{\partial t}=-\left(\frac{4\pi e n_0}{\varepsilon_0}\right)v(E)+D\frac{\partial^2 E}{\partial x^2}-v(E)\frac{\partial E}{\partial x}+\frac{4\pi}{\varepsilon_0}J(t), \tag{1}$$

where e is the electronic change, n_0 the equilibrium electron density, ε_0 the static dielectric constant, and D the diffusion constant. Here $v(E)$ is the electron drift velocity and $J(t)$ is the total current density. We Fourier-analyze $E(x, t)$ in the form

$$E(x, t)=E_0+\sum_{k\neq 0} c_k(t)\, e^{ik(x-v_0 t)}, \tag{2}$$

where E_0 is the applied electric field and $v_0=v(E_0)$. If the periodic boundary conditions are imposed on $E(x, t)$, the wave number k is given by $k=(2\pi/L)m$ as usual, in which L is the sample length and m are positive or negative integers except zero. It is convenient to label normal modes by m instead of k. Using Eq. (2) in Eq. (1), we obtain the system of coupled mode equations

$$\frac{dc_m}{dt}=\alpha_m c_m-\sum_{s=2}^{\infty}\sum_{(m_1+\cdots+m_s=m)}\frac{1}{s!}\left[\left(\frac{4\pi e n_0 v_0^{(s)}}{\varepsilon_0}\right)+ik_0 v_0^{(s-1)}m\right]c_{m_1}c_{m_2}\cdots c_{m_s}, \tag{3}$$

where $k_0=2\pi/L$ and $v_0^{(s)}=(d^s v(E)/dE^s)_{E=E_0}$. The growth rate α_m is given by $\alpha_m=(Dk_0^2)(p-m^2)$, with $p=-(4\pi e n_0 v_0^{(1)}/\varepsilon_0 D k_0^2)$, in which p is the parameter proportional to the negative differential mobility $-v_0^{(1)}$ and controls the instability of the system. When $p>1$, the modes satisfying the inequality $|m|<\sqrt{p}$ are amplified. The total current density $J(t)$ is expressed as

$$J(t)=J_0+\frac{1}{2}v_0^{(2)}\sum_m|c_m|^2+\frac{1}{6}v_0^{(3)}\sum_{(m+m'+m''=0)}c_m c_{m'}c_{m''}+\cdots, \tag{4}$$

where $J_0=en_0v_0$ is the ohmic current density.

In Eq. (3), we disregard all higher-order terms than four-mode coupling term ($s=3$) and take into account only such a coupling as $\sum_{m'}c_{m'}c_{-m'}c_m$ in this term, omitting the imaginary factor $ik_0v_0^{(2)}m$. For the numerical experiments, we consider a system of a finite number of modes whose maximum index is M, as illustrated in Fig. 1. It is convenient to introduce dimensionless time T by $T=(Dk_0^2\xi)t$, where $\xi=(p-1)$ for $p>1/2(M^2+1)$ and $\xi=(M^2-p)$ for $p<1/2(M^2+1)$. Furthermore, let us introduce dimensionless variables and quantities:

$$X_m=(V/Dk_0^2\xi)c_m,$$

$$g=Dk_0^2W/V^2, \quad a=-k_0v_0^{(1)}/V,$$

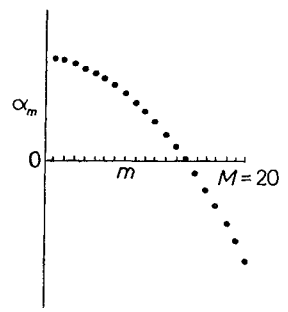

Fig. 1. The growth rate α_m as a function of m.

where

$$V=-(4\pi en_0 v_0^{(2)}/\varepsilon_0), \quad W=(4\pi en_0 v_0^{(3)}/\varepsilon_0).$$

In this approximation, Eq. (3) is reduced to

$$\dot{X}_m=\left[\left(\frac{p-m^2}{\xi}\right)-\xi g\sum_{m'=1}^{M}\left(1-\frac{1}{2}\delta_{m,m'}\right)|X_{m'}|^2\right]X_m+\frac{1}{2}(1+ima)\sum_{(m'+m''=m)}X_{m'}X_{m''}, \tag{5}$$

where the dot on X_m denotes differentiation with respect to T. For a typical sample of GaAs ($n_0=10^{15}\,\mathrm{cm}^{-3}$ and $L=10\,\mu m$), the modes up to at most $|m|=10$ are amplified in the negative mobility region. Then it will be sufficient to take $M=20$ as shown in Fig. 1.

Decomposing complex variables X_m into real and imaginary parts as $X_m=Y_{2m-1}+iY_{2m}$ for positive integers m, and using the relation $X_m=X_{-m}^*$ for negative integers m, we can write Eq. (5) in the form convenient for the numerical computations

$$\dot{Y}_{4n-3}=[\gamma_{2n-1}-\xi g(I-\tfrac{1}{2}Y_{4n-3}^2-\tfrac{1}{2}Y_{4n-2}^2)]Y_{4n-3}+(A_{2n-1}^{(r)}+B_{2n-1}^{(r)})-(2n-1)a(A_{2n-1}^{(i)}+B_{2n-1}^{(i)}), \tag{6a}$$

$$\dot{Y}_{4n-2}=[\gamma_{2n-1}-\xi g(I-\tfrac{1}{2}Y_{4n-3}^2-\tfrac{1}{2}Y_{4n-2}^2)]Y_{4n-2}+(A_{2n-1}^{(i)}+B_{2n-1}^{(i)})+(2n-1)a(A_{2n-1}^{(r)}+B_{2n-1}^{(r)}), \tag{6b}$$

$$\dot{Y}_{4n-1}=[\gamma_{2n}-\xi g(I-\tfrac{1}{2}Y_{4n-1}^2-\tfrac{1}{2}Y_{4n}^2)]Y_{4n-1}+(A_{2n}^{(r)}+B_{2n}^{(r)})-2na(A_{2n}^{(i)}+B_{2n}^{(i)})+\tfrac{1}{2}(Y_{2n-1}^2-Y_{2n}^2)-2naY_{2n-1}Y_{2n}, \tag{6c}$$

$$\dot{Y}_{4n}=[\gamma_{2n}-\xi g(I-\tfrac{1}{2}Y_{4n-1}^2-\tfrac{1}{2}Y_{4n}^2)]Y_{4n}+(A_{2n}^{(i)}+B_{2n}^{(i)})+2na(A_{2n}^{(r)}+B_{2n}^{(r)})+Y_{2n-1}Y_{2n}+na(Y_{2n-1}^2-Y_{2n}^2), \tag{6d}$$

for $n=1, 2, \cdots, 10$, where

$$\gamma_j=(p-j^2)/\xi, \tag{7}$$

$$I=\sum_{j=1}^{40}Y_j^2, \tag{8}$$

$$A_j^{(r)}=\sum_{l=1}^{20-j}(Y_{2l-1}Y_{2j+2l-1}+Y_{2l}Y_{2j+2l}), \tag{9a}$$

$$A_j^{(i)}=\sum_{l=1}^{20-j}(Y_{2l-1}Y_{2j+2l}-Y_{2l}Y_{2j+2l-1}), \tag{9b}$$

$$B_{2n-1}^{(r)}=\sum_{l=1}^{n-1}(Y_{2l-1}Y_{4n-2l-3}-Y_{2l}Y_{4n-2l-2}), \tag{10a}$$

$$B_{2n-1}^{(i)}=\sum_{l=1}^{n-1}(Y_{2l-1}Y_{4n-2l-2}+Y_{2l}Y_{4n-2l-3}), \tag{10b}$$

$$B_{2n}^{(r)}=\sum_{l=1}^{n-1}(Y_{2l-1}Y_{4n-2l-1}-Y_{2l}Y_{4n-2l}), \tag{11a}$$

$$B_{2n}^{(i)}=\sum_{l=1}^{n-1}(Y_{2l-1}Y_{4n-2l}+Y_{2l}Y_{4n-2l-1}), \tag{11b}$$

with the definition of $A_{20}^{(r)}=A_{20}^{(i)}=0$, $B_1^{(r)}=B_1^{(i)}=0$ and $B_2^{(r)}=B_2^{(i)}=0$. We must now treat the dynamical system of 40 modes.

Let us replace the nonlinear terms $B_{2n-1}^{(i)}$ on the right-hand sides of Eqs. (6a) and (6b) for $n=3, 4, \cdots, 10$ by new terms $\tilde{B}_{2n-1}^{(i)}$ defined as

$$\tilde{B}_{2n-1}^{(i)}=\sum_{l=1}^{n-1}(Y_{2n-1}Y_{4n-2l-2}+Y_{2l}Y_{4n-2l-3}), \tag{12}$$

which can be obtained by replacing Y_{2l-1} on the right-hand side of Eq. (10b) by $\dot{Y}_{2n-1}$. For $n=1, 2$, however, $B_1^{(i)}$ and $B_3^{(i)}$ remain unchanged. Thus, Eqs. (6) are rewritten as

$$\dot{Y}_{4n-3}=[\gamma_{2n-1}-\xi g(I-\tfrac{1}{2}Y_{4n-3}^2-\tfrac{1}{2}Y_{4n-2}^2)]Y_{4n-3}+(A_{2n-1}^{(r)}+B_{2n-1}^{(r)}) -(2n-1)a(A_{2n-1}^{(i)}+\tilde{B}_{2n-1}^{(i)}), \tag{13a}$$

$$\dot{Y}_{4n-2}=[\gamma_{2n-1}-\xi g(I-\tfrac{1}{2}Y_{4n-3}^2-\tfrac{1}{2}Y_{4n-2}^2)]Y_{4n-2}+(A_{2n-1}^{(i)}+\tilde{B}_{2n-1}^{(i)}) +(2n-1)a(A_{2n-1}^{(r)}+B_{2n-1}^{(r)}), \tag{13b}$$

$$\dot{Y}_{4n-1}=\text{the right-hand side of Eq. (6c)}, \tag{13c}$$

$$\dot{Y}_{4n}=\text{the right-hand side of Eq. (6d)}, \tag{13d}$$

for $n=1, 2, \cdots, 10$, with the definition of $\tilde{B}_1^{(i)}=B_1^{(i)}$ and $\tilde{B}_3^{(i)}=B_3^{(i)}$. Here, Eqs. (13c) and (13d) are the same as Eqs. (6c) and (6d). In the next section, we report the results of numerical experiments on the dynamical system of Eqs. (13).

§ 3. Results of computer experiments

We have solved numerically the system of Eqs. (13) by a standard Runge-Kutta-Gill integration routine. The dimensionless time increment was taken as $\Delta T=0.02$. In the experiment,[6] the current noise was measured. From Eq. (4), the current density J is determined in the lowest-order approximation by the quantity I defined by Eq. (8). Thus, a knowledge of the dynamics of the system may be obtained by investigating the time evolution of I.

(A) *Stochastic travel to a steady state*

Figure 2 shows the time behavior of I for $p=5000$, $g=0.002$ and $a=3.5$, with the initial conditions $Y_j(0)=0.1$ for all j $(=1, 2, \cdots, 40)$. In this case, all modes are amplified. Figure 3 presents the approach to an equilibrium point ($Y_j=0$ for all j) in an equilibrium state chosen as $p=-5000$, $g=0.002$ and $a=3.5$. As expected, the approach exhibits a monotonous decay with the relaxation time ~ 1 in the dimensionless time unit. However, the situation is changed completely in the negative mobility state ($p>1$), in which the equilibrium point becomes

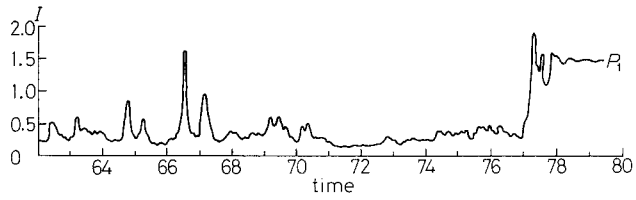

Fig. 2. Time evolution of I in an unstable state ($p=5000$, $g=0.002$ and $a=3.5$), where the initial conditions have been taken as $Y_j(0)=0.1$ for $j=1, 2, \cdots, 40$.

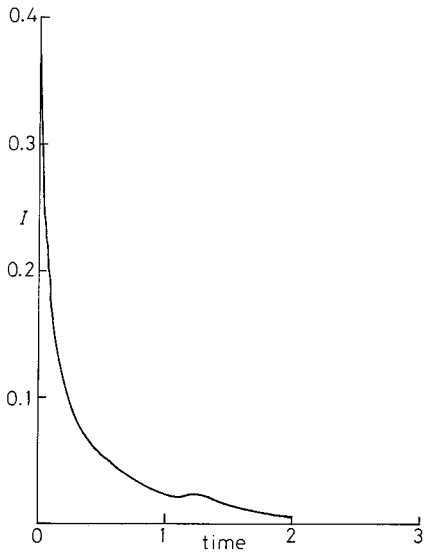

Fig. 3. Time evolution of I in an equilibrium state ($p=-5000$, $g=0.002$ and $a=3.5$), where the initial conditions are the same as those in Fig. 2.

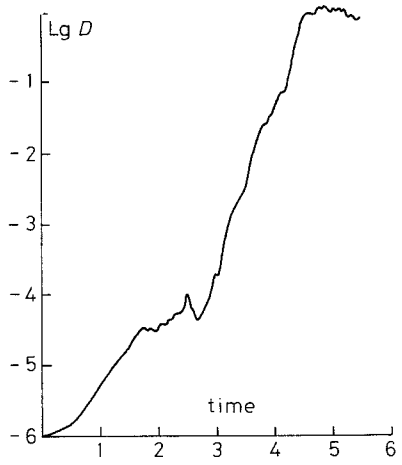

Fig. 4. Graph showing a typical curve of exponential growth in separation distance D between two trajectories starting with slightly differing initial conditions: (1) $Y_j(0)=0.01$ for all j, and (2) $Y_j(0)=0.01$ for $j=1, 2, \cdots, 39$, but $Y_{40}(0)=0.010001$. Here the numerical values of p, g and a are the same as those in Fig. 2.

unstable. Erratic or chaotic behavior continues for long time until the system reaches a steady state (attracting fixed point) P_1 from the unstable equilibrium point; in phase space the system exhibits a long-lived erratic trajectory in the approach to P_1. The life time of the erratic motion is ~ 77, which is much longer than the relaxation time ~ 1 in the equilibrium state. According to the modern ergodic theory,[12)~14)] the stochasticity of motion can be determined by investigating the growth in trajectory-pair separation distance. The theory states that trajectories are stochastic if initially close trajectory-pairs separate exponentially with time. This is called *stochastic* (or *exponential*) *instability*. In order to see the stochasticity of our long-lived erratic motion, we have computed the growth of separation distance D between two initially close trajectories in Fig. 4. One finds that D increases with time approximately in the exponential form: $D=D_0\exp(ht)$, where

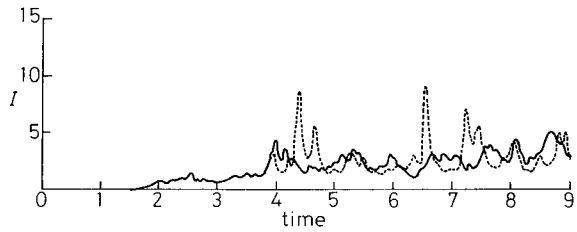

Fig. 5. Time behavior of two trajectories starting with slightly differing initial conditions; solid curve: $Y_j(0)=0.01$ for all j, and dotted curve: $Y_j(0)=0.01$ for $j=1, 2, \cdots, 39$, but $Y_{40}(0)=0.00999$. Here, $p=1000$, $g=0.002$ and $a=2.0$.

D_0 is the initial distance and h is the Kolmogorov-Sinai dynamical entropy. Thus, our erratic motion is certainly *stochastic*. The saturation behavior of D denotes that the stochastic region is bounded in phase space. However, we must mention that if initial conditions are set in the close vicinity of P_1, the approach to P_1 is of course monotonous, as in the equilibrium case, because P_1 is an attracting fixed point. Thus, *a small region around P_1 is not stochastic*. In Fig. 2, a giant peak is observed near $T=66.5$. Such peaks are generated irregularly. This suggests that our trajectorial flow is something like a single spiral whose outer portion returns after an appropriate twist toward the side of the same spiral with the outermost parts again facing the more central parts, as demonstrated by Rössler[18] as an example of a strange attractor. If the system trajectories obey the exponential law of growth of stochastic instability, two states differing by imperceptible amounts with respect to initial values $\{Y_j(0)\}$ must evolve eventually into two considerably different states, when the system starts with the equilibrium state. Figure 5 shows the time behavior of I for $p=1000$, $g=0.002$ and $a=2.0$, with two different initial conditions: (1) $Y_j(0)=0.01$ for all j, and (2) $Y_j(0)=0.01$ for $j=1, 2, \cdots, 39$, but $Y_{40}(0)=0.00999$. This case corresponds to the initial trajectory-pair separation distance $D_0=10^{-5}$. One sees that two trajectories exhibit completely different paths after a certain time$\sim$4. We may say that *stochastic trajectories are unstable with respect to small modifications of initial conditions*. It is impossible to give always the same value to $\{Y_j(0)\}$ because of thermal fluctuations inherent in the equilibrium state; there is any error whatever in observing the initial values $\{Y_j(0)\}$. Thus, whenever the same measurement is made repeatedly on the same sample under the same condition, observed states represented by points in phase space must be different from each other.*) *Although the basic equations* (13) *themselves are deterministic, a probabilistic*

*) In an example of Fig. 5, the system reached a limit cycle at $T\sim52$ for $Y_{40}(0)=0.01$ (see Fig. 10(a)) and two different fixed points at $T\sim80$ and 72 for $Y_{40}(0)=0.009999$ and 0.01000001, respectively. However the system trajectories were erratic even at $T=90$ for $Y_{40}(0)=0.00999$ and 0.010001. The fact that completely different final states appear by the small modifications of initial conditions is observed also in morphogenesis, (see R. Rosen, *Dynamical System Theory in Biology* (John Wiely and Sons, New York, 1970), Vol. I, Chap. 7.4).

approach is needed to understand the physical properties of their solutions. We confirmed that such stochastic trajectories appeared over a wide range of $p=10^2\sim10^4$. When there is no steady state (attractor), our stochastic motion must be identical with a strange attractor. *The system of Eqs.* (13) *provides an example of rigidly deterministic systems whose dynamics are best described in stochastic terms.* The importance of deterministic models with chaotic dynamics has been discussed by May[20] in the field of population biology.

(B) *Effect of external random forces*

Dissipative systems are always exposed by random forces through contact with a heat reservoir (or environmental causes). One will see that external random forces have an effect similar to that of initial conditions. These forces can be taken into account by adding εr_i to each right-hand side of Eqs. (13) (or in the form of a Langevin equation), where r_j is random numbers defined in the interval $[-1, 1]$ and ε is the parameter.[21] Our random forces do not obey the Gaussian distribution, but such a thing is not important for the study of their influence on system trajectories. Figure 6 shows the time evolution of I for the system applied by the random forces of $\varepsilon=10^{-5}$ under the same condition as that in Fig. 2. The system exhibits a stochastic trajectory with rather shorter life time ~44 to approach a new steady state (attracting fixed point) P_2. Figure 7 tells us that if initial conditions are the same, at the early stage a system exposed by random

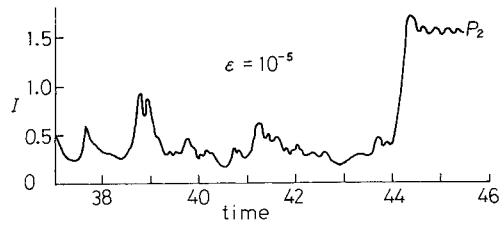

Fig. 6. Time evolution of I for the system applied by the random forces of $\varepsilon=10^{-5}$ under the same condition as that in Fig. 2.

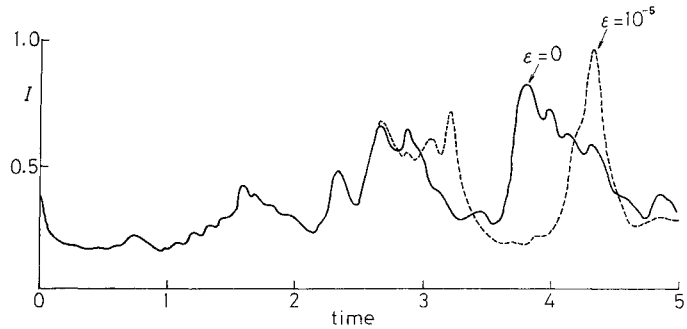

Fig. 7. Graph showing the influence of random forces on the trajectorial flow under the same condition as that in Fig. 2.

forces travels along almost the same trajectory as that of the system in the absence of random forces, but after some time two trajectories begin to separate from each other and at the later stage exhibit completely different paths. This behavior is quite similar to that in Fig. 5. This means that the influence of random forces accumulated gradually in the system during its travel along a trajectory provokes an unexpected change of the system after some time. In fact, in the case $\varepsilon=10^{-21}$, the system approached another steady state (attracting fixed point) P_3 after a long-lived stochastic travel. Thus, *stochastic trajectories are unstable with respect to small disturbances due to unknown environmental causes.* This behavior is closely related to the stochastic instability. There seems to be no "most probable path" in the approach to a steady state from the unstable equilibrium point.

(C) *Escape from a steady state*

As mentioned in the preceding subsection, our system possesses a number of steady states ($P_1, P_2, P_3, \cdots$) in the negative mobility state beyond the instability point and it reaches one of them via a long-lived stochastic travel from the unstable equilibrium state. Without external random forces, the system must stay eternally at this attractor. However, the situation is changed completely by the application of random forces. Figure 8 shows a time evolution of I for the system initially at P_1 under the application of random forces of $\varepsilon=1.8$. The system fluctuates around P_1 for a certain time ~ 27, and then escapes rather suddenly from P_1 to travel again along a stochastic trajectory. This trajectorial behavior is quite similar to that of $\varepsilon=0$ in Fig. 2. Thus, our motion is macroscopically stochastic. Figure 9 indicates that the duration of stay at the attractor depends sensitively on the strength, ε, of random forces. We may say that the influence of random forces accumulated gradually in the system gives eventually rise to its escape from the attractor, as expected from Fig. 7. This is an important effect. Figure 10 shows also the approach to an attracting closed orbit (limit cycle) for $p=1000$, $g=0.002$, $a=2.0$ and $\varepsilon=0$, with the initial conditions $Y_j(0)=0.01$ for all j, and the escape from it under the application of random forces of $\varepsilon=2.0$. The experiments showed that the system possessed two more attracting fixed points.

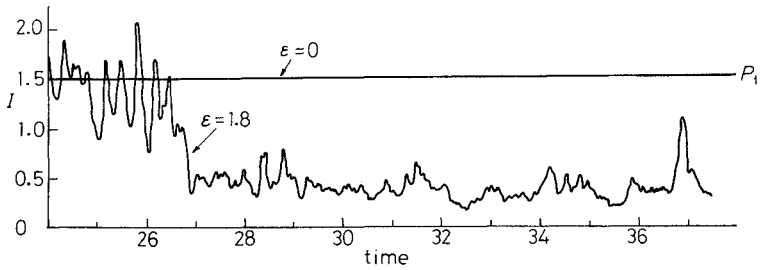

Fig. 8. This graph shows clearly that the system can escape from the attractor P_1 under the application of random forces; $p=5000$, $g=0.002$, $a=3.5$ and $\varepsilon=1.8$.

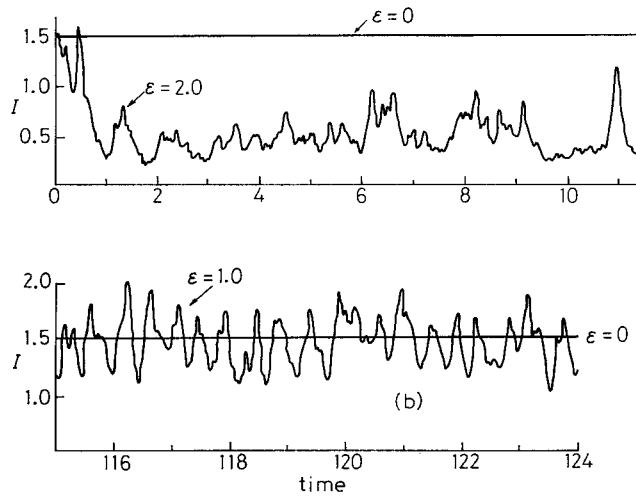

Fig. 9. The ε-dependence of the duration of stay at P_1.

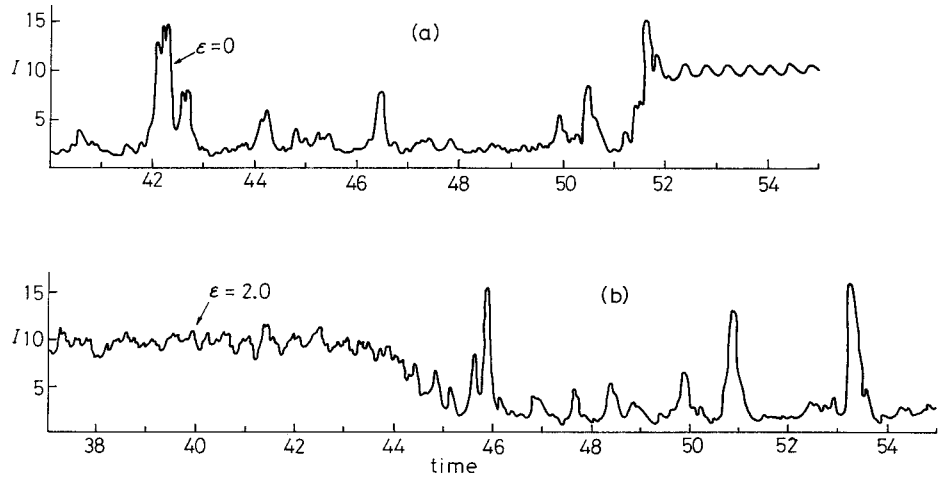

Fig. 10. Time evolution of I in an unstable state ($p=1000$, $g=0.002$ and $a=2.0$). (a) Approach to a limit cycle; the initial conditions $Y_j(0)=0.01$ for all j. (b) Escape from the limit cycle under the application of random forces of $\varepsilon=2.0$.

§ 4. Discussion

Our computer experiments indicate that there are three interesting phenomena associated with instability in a dissipative system. First, the system exhibits a long-lived stochastic trajectory in its travel to a steady state from the unstable equilibrium point. Stochastic trajectories are unstable with respect to external disturbances. This is closely related to the exponential law of growth of stochastic instability. Since these trajectories are obtained without introducing external sto-

chastic elements into the basic equations, the motion described by them is macroscopic. Thus, our system provides an example of fully deterministic systems whose dynamics are best described probabilistically. If the system stays eternally at the reached attractor, the long-lived stochastic motion on the way to the attractor will be observed simply as a large enhancement of fluctuations in a transient phenomena. Such an enhancement effect was discussed by many investigators in connection with the transient statistical properties of a laser, superradiance and electrical oscillation. In particular, Suzuki[22] has recently developed a scaling theory of transient fluctuations. However, the problems discussed by them seem to be essentially different from ours, because in these cases the enhancement effect does not come from the nonlinearity inherent in the system, as in our case, but from the nonlinear transformation of external random forces. In fact, since the solutions of an equation of motion $\dot{X}=X(p-X)$, which presents a good model for a laser and has been adopted by Suzuki as an example for the fluctuation-enhancement effect, exhibit always a monotonic decay to a steady state from an unstable equilibrium point ($p>0$) and do not show any stochastic behavior, there is no fluctuation in the absence of external random forces, from our viewpoint. Now, the situation is changed completely by the application of random forces. Secondly, under their influence, the system can escape from the attractor after fluctuating around it for some time. *The escape effect never occurred in the equilibrium state.* Thirdly, the system travels again along a stochastic trajectory after its escape from the attractor. We confirmed that these three phenomena occur over a wide range of $p=10^2\sim10^4$. From these results, we conclude that the system wanders erratically from attractor to attractor via long-lived stochastic trajectories. This wandering motion looks seemingly like a strange attractor in a sense that there is no stable point to stay eternally. We must now emphasize that the wandering motion is provoked by the external random forces, but its stochasticity is governed by the macroscopic motion arising from the nonlinearity inherent in the system. This is in contrast with the thermal fluctuations in equilibrium systems, whose magnitude varies in proportion to the strength of external random forces. Thus, the wandering motion will be observed as large fluctuations. If a system possesses a single steady state beyond the instability point, stochastic trajectories may be viewed as long-lived excitations in the steady state. Then, it is easily understood that the very existence of these excitations enhances anomalously fluctuations, as compared with short-lived excitations in the equilibrium state. We may say that the concept of a strange attractor corresponds to a special case, in which there is no attractor, to our wandering motion. Generally speaking, however, it is not so easy to obtain wandering solutions. We could not find any stochastic motion for small values of a. For example, for $p=100$, $g=0.04$ and $a=0$, the system trajectory was similar to that in the equilibrium state. However, when $a=2.5$, the system trajectory was again stochastic. For $p=10^4$, $g=0.002$ and $a=2.0$, the system (13) completed a closed orbit with short relaxation time. Our numerical analysis show-

ed that the system could not escape from the orbit even under the application of random forces of $\varepsilon=5.0$ and fluctuated around it as if the orbit was crushed. Our computer experiments indicated that *an attractor was stable under the application of random forces if the approach to it from the unstable equilibrium point exhibited a monotonic decay with short relaxation time* ~ 1, *while it became unstable if the approach exhibited a long-lived stochastic behavior.* Figuratively speaking in topographyical terms, the former case is compared to the motion of a ball in a deep valley whose slope is steeply rising, while the latter one is compared to its motion on a basin (like a frying pan or a billiard table) possessing a number of shallow traps.

One may say that our dynamical system (13) is rather unrealistic in a sense that a part of actual nonlinear interactions has been replaced by artificial forms, or that it has, as a model of a model, no longer an immediate physical interpretation. However, the discovered phenomena are natural from the physical point of view. Therefore, we may say that these phenomena are generic and characteristic of instabilities in dissipative systems. We propose our wandering motion as a candidate for the mechanism of anomalous fluctuations. Then, the following questions will be raised. How long does the system stay at an attractor? Which attractor does the system reach after escaping from this attractor? How long does the system travel along a stochastic trajectory? These questions must be answered on the basis of a statistical concept.

Acknowledgement

The author would like to thank Dr. K. Matsuno for useful discussions.

References

1) E. R. Pike, D. A. Jackson, P. J. Bourke and D. I. Page, J. Phys. **E1** (1968), 727.
2) G. Ahlers, Phys. Rev. Letters **33** (1974), 1185.
3) J. P. Gollub and H. L. Swinney, Phys. Rev. Letters **35** (1975), 927.
4) H. B. Møller and T. Riste, Phys. Rev. Letters **34** (1975), 996.
5) S. Kai, M. Araoka, H. Yamazaki and K. Hirakawa, J. Phys. Soc. Japan **40** (1976), 305.
6) K. Matsuno, Phys. Letters **31A** (1970), 335.
7) S. Kabashima, H. Yamazaki and T. Kawakubo, J. Phys. Soc. Japan **40** (1976), 921.
8) A. R. Moore, J. Appl. Phys. **38** (1967), 2327.
9) P. A. Gielen and R. J. J. Zijlstra, Solid State Comm. **18** (1976), 1009.
10) T. L. Paoli, IEEE J. Quantum Electron. **QE11** (1975), 276.
11) E. N. Lorenz, J. Atmos. Sci. **20** (1963), 130.
12) Ja. G. Sinai, Russ. Math. Surv. **25** (1970), 137.
13) J. Ford, Adv. Chem. Phys. **24** (1973), 155; in *Fundamental Problems in Statistical Mechanics*, III, edited by E. G. D. Cohen (North-Holland Amsterdam, 1975).
14) B. V. Chirikov, F. M. Izrailev and V. A. Tayursky, Comput. Phys. Comm. **5** (1973), 11.
15) D. Ruelle and F. Takens, Comm. Math. Phys. **20** (1971), 167.
16) J. B. McLaughlin and P. Martin, Phys. Rev. **A12** (1975), 186.
17) O. E. Rössler, Z. Naturforsch. **31a** (1976), 259.
18) O. E. Rössler, Phys. Letters **57A** (1976), 397.
19) K. Nakamura, J. Phys. Soc. Japan **38** (1975), 46.
20) R. M. May, Nature **256** (1975), 165; J. Theor. Biol. **51** (1975), 511.
21) K. Matsuno, Phys. Rev. **A11** (1975), 1016.
22) M. Suzuki, Prog. Theor. Phys. **56** (1976), 77, 477.